

## MINERALOGICAL AND GEOCHEMICAL STUDY OF ANDESITE ALTERATION ZONE IN BUKIT MANTRI GOLD MINE, BALUNG, SABAH

Mohd Shafreen Mad Isa<sup>1</sup> and Baba Musta<sup>2</sup>

<sup>1,2</sup> Faculty of Science and Natural Resources,  
University Malaysia Sabah, Malaysia, Jalan UMS, 88400 Kota Kinabalu, Sabah, Malaysia

Email: [shafreen@live.com.my](mailto:shafreen@live.com.my)<sup>1</sup>, [babamus@ums.edu.my](mailto:babamus@ums.edu.my)<sup>2</sup>

Received 09<sup>th</sup> September 2022; accepted 8<sup>th</sup> February 2023

Available online 20<sup>th</sup> April 2023

Doi: <https://doi.org/10.51200/bsj.v44i1.4347>

**ABSTRACT:** *This paper highlights the geochemical compositions and mineralogy of the alteration zone of the andesitic host rock and volcanic breccia in Bukit Mantri area near Balung, Tawau, Sabah, where a gold mining project is now taking place. Minerals identified by XRD analysis include quartz, pyrite, K-feldspar, muscovite, chlorite, kaolinite, hematite, and goethite, while thin section analysis confirms the abundance of pyrite. XRF and ICP-OES analyses suggest a significant concentration of SO<sub>3</sub>, Cu, Pb, Zn and As, with average values of 2.68wt%, 254µg/g, 236.9µg/g, 232.9µg/g, and 30.6µg/g, respectively, in the hydrothermally altered andesite. The widespread presence of pyrite and higher concentration of SO<sub>3</sub> provide insights for environmental control for its higher acidity generation potential. Meanwhile, secondary minerals such as iron and aluminium oxides and silicate minerals may provide acid buffers and reduce the dispersion of constituents.*

**KEYWORDS:** geochemistry, mineralogy, hydrothermal alterations, gold mineralisation, Bukit Mantri

### INTRODUCTION

A mining lease was issued for a gold mining project in 2013 and began developing its mine between 2017 and 2018 in Bukit Mantri, near Balung, Tawau, Sabah. The approved mining lease is situated between Bukit Mantri and Bukit Tundong, geographically bounded by 4°29'N to 4°31'N and 118°6'E to 118°8'E, near Balung, Tawau, Sabah (Figure 1). The first phase of mine development and mining activities focuses on the Bukit Mantri area.

The geology of the area is characterised by andesitic to dacitic volcanic flow and pyroclastic of Pliocene, and Kalumpang Formation, which consists of marine sediments interbedded with volcanoclastics composed of tuff, sandstone, claystone, volcanic conglomerates and breccia, and limestone, and deposited in an early Middle Miocene shallow neritic environment (Musta et al., 2008; Tahir et al., 2010).

The volcanic hosts an epithermal low-sulphidation gold deposit (Haruna, 2016; Yan, 1991), and the mineralisation is described as a series of quartz-sulphide hydrothermal breccia veins enveloped by quartz-adularia-sericite near the veins, argillic, and propylitic alterations. Other reported alteration profiles include silicic, late-stage kaolinitic, and late-stage carbonate. These wall-rock alterations indicate the changes in geochemical composition and mineralogy of host rock (Nordstrom, 2011) and potentially affect the surrounding environment as they both can increase and decrease acid-generating capacity (Plumlee, 1999).

Moreover, oxidations, formation of secondary minerals and sorption could also superimpose the variability of the geochemical composition of the mineral deposits and host rocks (Nordstrom & Alpers, 1999; Plumlee, 1999; Smith, 1999).

Presently, the background geochemical composition and mineralisation, and their relationship to hydrothermal mineralisation and dispersion, are unavailable. Therefore, the objectives of this study are to examine the geochemical composition of hydrothermally altered host rocks and volcanic breccia in the area and to discover signature minerals that may have an impact on the environment.

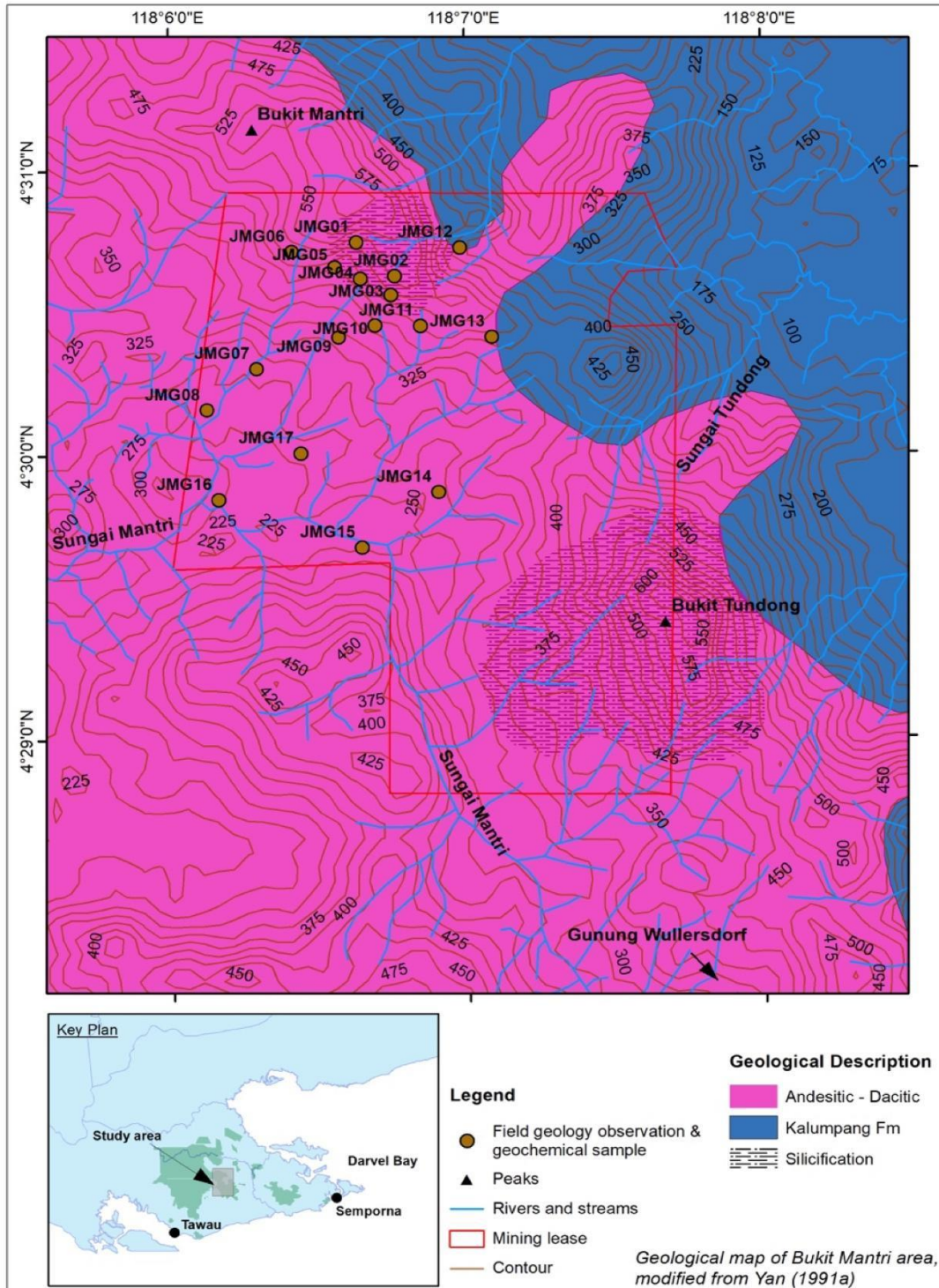


**Figure 1. The geological map of the study area based on Yan (1991) and the distribution of sampling locations.**



## MATERIALS AND METHODS

Seventeen hand specimen samples of the alteration zone of andesitic rock were collected from fresh outcrops in the surrounding area of Bukit Mantri during the early phase of mine development in May 2018 (Figure 2), and they are identified as argillised, propylitised, silicified, argilised and sulphidised andesite, and volcanic breccia. The descriptions of the hand specimens are listed in Table 1.

Selected hand specimens of argilised, propylitised and silicified andesite were cut, placed on glass, and polished to a thickness of about 0.03 mm for thin section analysis (Figure 3), and the identification of minerals is based on Mackenzie et al. (2017). Meanwhile, crushed and pulverised samples were then used for mineral identification by X-Ray Diffraction (XRD) technique using Cu-source X-Ray, measuring at diffraction angle,  $2\theta$  between  $10^\circ$  and  $80^\circ$  for about 30 minutes using Bruker D8 Advance (Bruker Corp.), subsequently analysed using High Score Plus Version 3.0.5 application (Malvern Panalytical Inc.) with The American Mineralogist Crystal Structure Database as the reference (Clark & Downs, 2004; Downs & Hall-Wallace, 2003).

Major elements geochemistry was analysed using pre-prepared fuse discs from the pulverised samples with X-Ray Fluorescence (XRF) Spectrometer (Musta et al., 2008) using PANalytical Zetium XRF Spectrometer (Malvern Panalytical Inc.). In contrast, trace elements were measured using Inductively Coupled Plasma - Optical Emission Spectrometry (ICP-OES) technique using Perkin Elmer Optima 5300 DV Spectrometer (PerkinElmer Inc.). Prior to ICP-OES analysis, samples were digested with 70% concentrated  $\text{HNO}_3$  and 50% concentrated HF inside Teflon beakers under slow heating between  $90^\circ\text{C}$  and  $100^\circ\text{C}$  on a hotplate. Loss on Ignition (LOI) was performed gravimetrically and incorporated for the total of major elements geochemistry calculation. General statistical and coefficient of correlation analysis ( $r$ ) calculations were performed in Microsoft Excel 365 (Microsoft Corp.).







**Figure 2. Outcrops and hand specimen samples in the alteration zone of andesite and volcanic breccia in Bukit Mantri area; (a) and (b) argillised andesite, (c) and (d) propylitised andesite, (e) and (f) silicified andesite, (g) and (h) volcanic breccia, and (i) and (j) argillised and sulphidised andesite.**

**Table 1. Description of hand specimens of hydrothermally altered andesite and volcanic breccia in Bukit Mantri area**

ID	Description of hand specimen	ID	Description of hand specimen
JMG-01	Weak to moderately argillised andesite, yellowish — purplish dark brown, moderate to highly oxidised and weathered, moderately limonitic, ferromanganese (Fe-Mn) was observed in some parts, mostly along with the fractures, and no sulphides were noted.	JMG-02	Weakly argillised andesite, yellowish — purplish dark brown, moderate to highly oxidised and weathered, moderately limonitic with few ferromanganeses (Fe-Mn) along the fractures, cut by weak — moderately intense quartz veinlets, and disseminated relics of fine-grained sulphides observed most likely pyrite.
JMG-03	Moderately argillised andesite. Whitish to yellowish, highly oxidised and weathered, moderately limonitic with few ferromanganeses (Fe-Mn) along the fractures, relics of fine-grained pyrite observed in some parts	JMG-04	Moderate to highly argillised andesite, whitish to purplish, highly oxidised and weathered, moderately limonitic, moderately cut by quartz veins.
JMG-05	Prophylic andesite, slightly weathered to fresh, greenish grey, moderate to strongly chloritised, cut by few limonitic quartz veins, dissemination of fine-grained pyrite and few chalcopyrite observed pervasively.	JMG-06	Prophylic andesite, slightly weathered to fresh, greenish grey, porphyritic with phenocryst of feldspar, weak to moderately chloritised, dissemination of fine-grained pyrite noted.
JMG-07	Moderate to highly weathered and oxidised andesite, purplish to whitish-yellow, moderately argilised, limonite observed mostly along fractures, pyrite relics noted in some parts.	JMG-08	Moderate to highly weathered and oxidised andesite, yellowish to purplish brown, weak to moderately limonitic and hematitic mostly along fractures, relics of sulphides noted in some parts.
JMG-11	Moderate to strongly argillised andesite, whitish - greenish grey, chloritic, moderately to highly oxidised and weathered, moderately limonitic with the dissemination of fine-grained pyrite observed.	JMG-12	Volcanic breccia/Volcanoclastic with angular to subangular volcanic rock clasts, yellowish to reddish-brown, highly weathered and oxidised, cut by weakly intense ferromanganese (Fe-Mn) veins, no sulphides observed.
JMG-13	Highly weathered and oxidised propylitised andesite, yellowish to purplish brown, clayey, cut by weakly intense ferromanganese (Fe-Mn) veins, no sulphides observed.	JMG-14	Moderate to highly sulphidised and argillised andesite, highly weathered and oxidised, greenish – whitish light grey, dissemination of fine to medium-grained pyrite observed pervasively.

ID	Description of hand specimen	ID	Description of hand specimen
JMG-15	Moderate to highly sulphidised and argilised Andesite, moderately to highly weathered and oxidised, greenish — whitish light grey, disseminating fine to medium-grained pyrite observed pervasively.	JMG-16	Moderate to highly sulphidised and argilised andesite, greenish — whitish light grey, moderately to highly weathered and oxidised, cut by weak to moderately intense limonitic quartz veins, dissemination of fine to medium-grained pyrite observed pervasively.
JMG-17	Moderate to highly sulphidised and argilised andesite, greenish — whitish light grey, moderately to highly weathered and oxidised, limonitic quartz veins noted in few parts, dissemination of fine to medium-grained pyrite observed pervasively.		

## RESULTS & DISCUSSION

### *Mineralogy*

Quartz, pyrite, muscovite, K-feldspar, chlorite, goethite, hematite, and kaolinite are minerals that appear in XRD spectrograms (Figure 4). Pyrite becomes a major mineral after quartz, appearing in argillised, propylitised, silicified, sulphidised and argillised andesite. Muscovite is found in sulphidised and argillised andesite, whereas K-feldspar and chlorite are identified in propylitised andesite. Additionally, goethite, hematite, and kaolinite are also presented, and these secondary minerals are the results of weathering on the country rocks.

The specimens' micrographs under plane-polarised light (PPL) and cross-polarised light (XPL) confirm the presence of quartz, pyrite, K-feldspar and chlorite (Figure 3). Pyrite has been observed in all specimens, including propylitised andesite, indicated by dark (opaque) and cubical-shaped crystals in the optical micrographs. Meanwhile, K-feldspar, chlorite, and mineral crystals of unidentified sulphide minerals that appeared alongside pyrite are observed in propylitic and argillised andesite, respectively. In the prospecting and earlier geochemical survey reports, some notable sulphide minerals are chalcopyrite, sphalerite and galena, while muscovite and K-feldspar are referred to as sericite and adularia, respectively (Haruna, 2016; Yan, 1991). The analyses on XRD spectrograms and thin section microscopy suggest that pyrite is highly distributed in host rocks and has become the principal mineral of environmental concern owing to its potential to increase acid-producing capacity. Meanwhile, the availability of silicate and secondary minerals in the area could attenuate acid waters and limit trace elements' mobility.



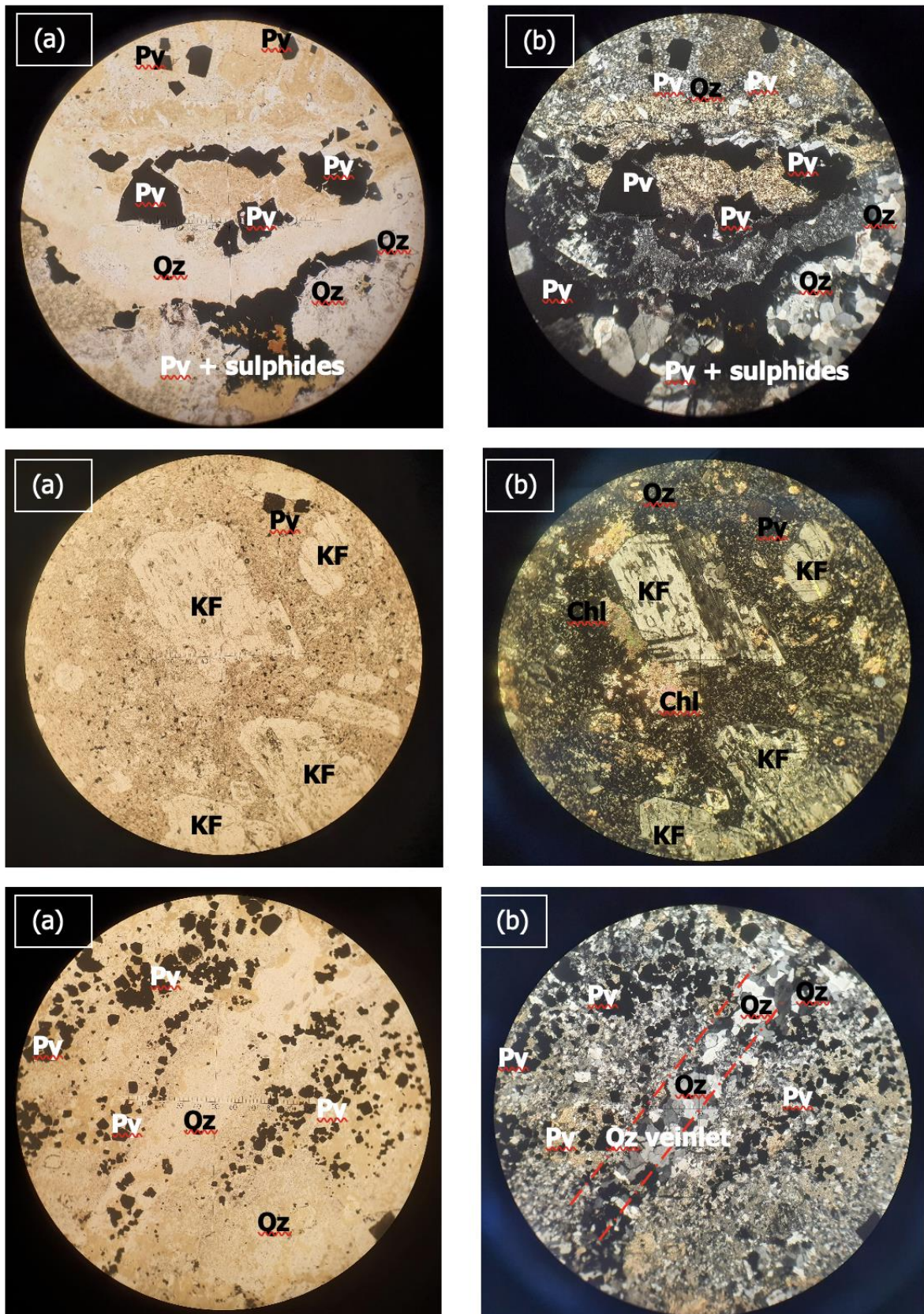
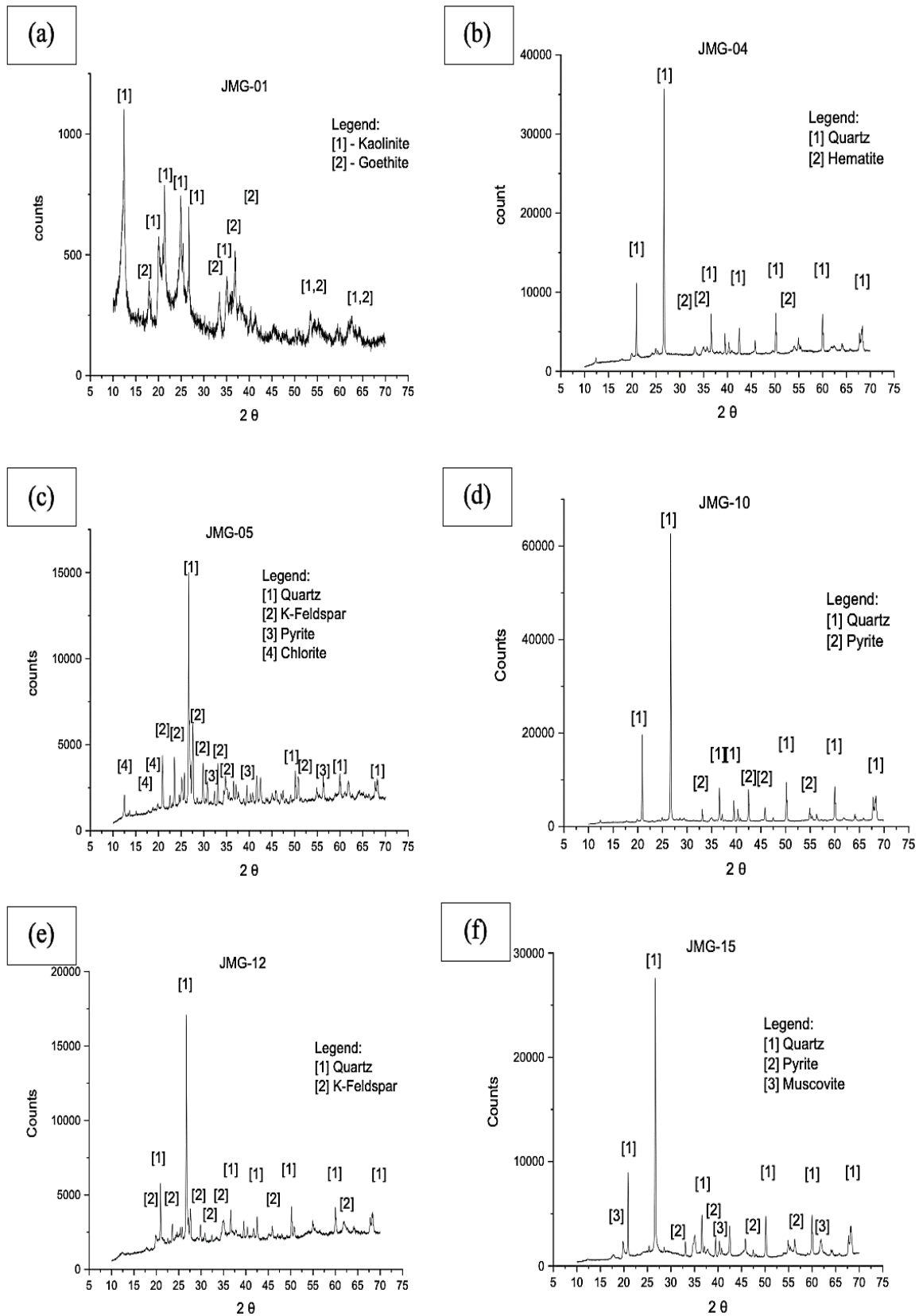


Figure 3. Thin section optical microscopy images of selected hydrothermally altered andesite; (a) argillised andesite (PPL), (b) argillised andesite (XPL), (c) propylitised andesite (PPL), (d) propylitised andesite (XPL), (e) silicified andesite (PPL), and (f) silicified andesite (XPL), showing the presence of quartz (Qz), pyrite (py), K-feldspar (KF), and chlorite (Chl).



**Figure 4. XRD Spectrograms show mineral phases identified as [a] kaolinite and goethite in highly weathered argilised andesite, [b] quartz and hematite in weathered argilised andesite, [c] quartz, K-feldspar, pyrite, and chlorite in propylitised andesite, [d] quartz and pyrite in silicified andesite, [e] quartz and K-feldspar in volcanic breccia, and [f] quartz, pyrite, and muscovite in sulphidised and argilised andesite.**



***Major elements geochemistry***

Tables 2 and 3 summarise the results of major element geochemistry and the calculation results of coefficient of correlations among the major elements. SiO<sub>2</sub> is the most abundant oxide in the country rocks, ranging from 32.77wt% to 74.39wt%. Al<sub>2</sub>O<sub>3</sub> and Fe<sub>2</sub>O<sub>3</sub><sup>T</sup> are the second and third most abundant oxides, between 6.11wt% and 26.00wt%, 3.73wt% and 23.45wt%, respectively. The oxide of other major elements such as TiO<sub>2</sub>, K<sub>2</sub>O, MnO, MgO, CaO, Na<sub>2</sub>O and P<sub>2</sub>O<sub>5</sub> made up the rest of the geochemical compositions, from below the detection limit to 7.52wt%. Meanwhile, SO<sub>3</sub> is ranging 0.03wt% to 7.35wt%, and LOI from 3.28wt% to 13.45wt%.

Silicified andesite has the most SiO<sub>2</sub>. During silicification, rock materials have been replaced by SiO<sub>2</sub> (Plumlee, 1999), resulting in a higher SiO<sub>2</sub> concentration. SiO<sub>2</sub> has a moderate to strong negative correlation with Al<sub>2</sub>O<sub>3</sub> and Fe<sub>2</sub>O<sub>3</sub><sup>T</sup> ( $r=-0.80$  and  $r=-0.75$ ), suggesting the formation of secondary minerals containing these oxides are likely to form as the degree of weathering increases while the concentration of SiO<sub>2</sub> decreases. The average Fe<sub>2</sub>O<sub>3</sub><sup>T</sup> composition of all andesite samples is 8.56wt%, relatively higher than the reference composition, 3.27wt% (Winter, 2014), indicating that the country rock has relatively weathered.

The average concentration of MgO, CaO and Na<sub>2</sub>O in the hydrothermally altered andesite are 1.03wt%, 0.09wt%, and 0.06wt%, respectively, which appear to be lower than their respective reference compositions of 3.33wt%, 6.79wt%, and 4.48wt%, whereas K<sub>2</sub>O and MnO are 3.36wt% and 0.41wt%, respectively have increased from 1.62wt% and 0.14wt%. The near-zero correlation of MgO, CaO and Na<sub>2</sub>O with Al<sub>2</sub>O<sub>3</sub> and Fe<sub>2</sub>O<sub>3</sub><sup>T</sup> suggests the leaching of these oxides during weathering is relatively weak but varying due to hydrothermal alterations. MgO and CaO are also relatively higher in propylitised andesite than in other alteration profiles of andesite and volcanic breccia. The relatively higher average of K<sub>2</sub>O than the reference composition and the relatively higher concentration in propylitic andesite and volcanic breccia suggest hydrothermal alterations have introduced and enriched potassium-bearing minerals such as K-feldspar or adularia in the parent rocks.

**Table 2. The concentration of major elements in hydrothermally altered andesite and volcanic breccia in Bukit Mantri gold mine area, Tawau, Sabah.**

Id	Rock Type <sup>alt.</sup>	SiO <sub>2</sub>	TiO <sub>2</sub>	Al <sub>2</sub> O <sub>3</sub>	Fe <sub>2</sub> O <sub>3</sub> <sup>T</sup>	MnO	MgO	CaO	Na <sub>2</sub> O	K <sub>2</sub> O	P <sub>2</sub> O <sub>5</sub>	SO <sub>3</sub>	LOI	TOTAL
		wt%												
JMG-01	And. <sup>arg.</sup>	32.77	1.01	26.00	23.45	1.49	0.17	0.00	0.02	1.11	0.14	0.38	13.45	100.00
JMG-02	And. <sup>arg.</sup>	74.39	0.61	12.99	4.82	0.03	0.46	0.03	0.06	2.90	0.05	0.36	3.28	100.00
JMG-03	And. <sup>arg.</sup>	56.80	0.72	18.51	10.72	2.07	0.77	0.02	0.05	3.52	0.03	0.11	6.68	100.00
JMG-04	And. <sup>arg.</sup>	66.56	0.61	14.13	10.80	0.03	0.37	0.01	0.02	1.80	0.03	0.17	5.47	100.00
JMG-05	And. <sup>prop.</sup>	53.81	0.57	14.82	8.76	0.42	1.49	0.04	0.13	7.32	0.03	6.16	6.46	100.00
JMG-06	And. <sup>prop.</sup>	61.62	0.64	15.28	7.36	0.91	3.34	1.05	0.07	4.63	0.10	0.30	4.71	100.00
JMG-07	And. <sup>arg.</sup>	66.76	0.75	19.67	3.73	0.02	0.53	0.03	0.04	2.94	0.01	0.03	5.49	100.00
JMG-08	And. <sup>prop.</sup>	60.43	0.70	17.89	10.21	0.03	0.66	0.01	0.02	2.70	0.02	0.09	7.26	100.00
JMG-09	And. <sup>arg.</sup>	61.70	0.64	14.80	7.46	0.03	0.76	0.02	0.09	2.97	0.03	0.31	11.18	100.00
JMG-10	And. <sup>si.</sup>	74.14	0.20	6.11	6.34	0.04	0.13	0.04	0.01	1.14	0.02	6.06	5.77	100.00
JMG-11	And. <sup>arg.</sup>	55.04	0.83	17.98	10.51	0.26	1.57	0.06	0.14	3.04	0.10	3.53	6.96	100.00
JMG-12	Volc. Breccia	58.04	0.94	18.91	8.93	0.94	0.47	0.03	0.08	4.68	0.08	0.07	6.84	100.00
JMG-13	And. <sup>prop.</sup>	48.43	1.05	23.90	9.93	1.04	0.15	0.01	0.12	7.52	0.04	0.13	7.67	100.00
JMG-14	And. <sup>arg., sulph.</sup>	62.05	0.52	14.59	5.24	0.05	0.86	0.06	0.04	3.70	0.01	5.52	7.37	100.00
JMG-15	And. <sup>arg., sulph.</sup>	60.58	0.65	16.78	4.57	0.02	1.07	0.02	0.03	3.28	0.02	5.37	7.61	100.00
JMG-16	And. <sup>arg., sulph.</sup>	54.39	0.59	16.12	6.59	0.07	3.15	0.02	0.09	1.55	0.03	7.35	10.05	100.00
JMG-17	And. <sup>arg., sulph.</sup>	51.85	0.56	17.12	6.49	0.03	0.95	0.03	0.08	3.62	0.03	6.98	12.27	100.00
Minimum		32.77	0.20	6.11	3.73	0.02	0.13	0.00	0.01	1.11	0.01	0.03	3.28	
Maximum		74.39	1.05	26.00	23.45	2.07	3.34	1.05	0.14	7.52	0.14	7.35	13.45	
Average <sup>1</sup> , $\bar{x}$		58.83	0.67	16.67	8.56	0.41	1.03	0.09	0.06	3.36	0.04	2.68	7.61	
Ref. comp.		57.9	0.87	17.0	3.27	0.14	3.33	6.79	3.48	1.62				99.27 <sup>2</sup>

Remarks: Alt = alteration, And = andesite, arg. = argilised, prop. = propylitised, si. = silicified, sulph. = sulphidised, bdl = below detection limit, Ref. comp. = ref composition. The geochemical compositions are normalised to 100 wt%. <sup>1</sup> = average exclude of volcanic breccia, <sup>2</sup> = include H<sub>2</sub>O composition of 0.83%. Reference andesite geochemical composition: Winter (2014).



**Table 3. The coefficient of correlations, r between major elements.**

Item	TiO <sub>2</sub>	Al <sub>2</sub> O <sub>3</sub>	Fe <sub>2</sub> O <sub>3</sub> <sup>T</sup>	MnO	MgO	CaO	Na <sub>2</sub> O	K <sub>2</sub> O	P <sub>2</sub> O <sub>5</sub>	SO <sub>3</sub>	LOI
SiO <sub>2</sub>	-0.66	-0.80	-0.75	-0.55	-0.05	0.10	-0.28	-0.18	-0.55	-0.01	-0.74
TiO <sub>2</sub>		0.93	0.55	0.55	-0.16	-0.08	0.31	0.32	0.55	-0.58	0.25
Al <sub>2</sub> O <sub>3</sub>			0.59	0.55	-0.13	-0.12	0.19	0.24	0.45	-0.41	0.45
Fe <sub>2</sub> O <sub>3</sub> <sup>T</sup>				0.61	-0.23	-0.10	-0.09	-0.17	0.70	-0.33	0.49
MnO					-0.06	0.17	0.07	0.24	0.50	-0.43	0.12
MgO						0.65	0.37	0.07	0.16	0.33	-0.03
CaO							0.06	0.18	0.37	-0.16	-0.29
Na <sub>2</sub> O								0.65	0.18	0.16	0.07
K <sub>2</sub> O									-0.07	-0.05	-0.20
P <sub>2</sub> O <sub>5</sub>										-0.32	0.22
SO <sub>3</sub>											0.24

SO<sub>3</sub> is consistently higher in argilised and sulphidised andesite, and its concentration is also significant in some argilised, propylitised and silicified andesite, whereas it is least in volcanic breccia. It is anticipated that the sulphidation process has fundamentally altered the geochemistry and increased the concentration of sulphide minerals, especially pyrite. LOI was found in high concentrations in the parent rocks. The coefficient of correlation between LOI and SiO<sub>2</sub> shows a negative and moderate relationship ( $r = -0.74$ ), implying it also shows volatile matters such as sulphur gases in sulphidised samples are likely higher in weathered materials than in relatively fresh parent rocks.

#### *Trace elements geochemistry*

Results of ICP-OES on trace element geochemistry are tabulated in Table 4. The concentration of trace elements, i.e. As, Ba, Cu, Pb, Zn, Cd, Cr, Ni, and Ag are 8.1µg/g to 129.2µg/g, 101.0µg/g to 103.8µg/g, 9.1µg/g to 827.1µg/g, 12.2µg/g to 535.3µg/g, 61.2µg/g to 929.9µg/g, below detection limit to 4.2µg/g, 11µg/g to 27.µg/g, 4.2µg/g to 16.9µg/g, and below detection limit to 2.6µg/g, respectively. The most significant trace elements in the parent rocks are Cu, Pb, Zn and As. On average, the Cu, Pb and Zn concentrations are nearly identical in the altered andesite of 254.0µg/g, 236.9µg/g and 232.9µg/g, respectively. On the contrary, in volcanic breccia, Cu concentration is significantly lower, 42.1µg/g, than Pb, 535.3µg/g and Zn, 541.2µg/g, respectively.

**Table 4. The concentration of trace elements in the hydrothermally altered andesite and volcanic breccia in Bukit Mantri gold mine area, Tawau, Sabah.**

Id	Rock Type <sup>alt.</sup>	As	Ba	Cu	Pb	Zn	Cd	Cr	Ni	Ag
		µg/g								
JMG-01	And. <sup>arg.</sup>	25.4	102.7	131.2	430.1	548.7	0.2	15.5	6.5	<0.01
JMG-02	And. <sup>arg.</sup>	30.9	101.4	40.4	486.2	72	0.2	11.4	4.2	2.6
JMG-03	And. <sup>arg.</sup>	108.5	101	351.2	427	246.5	1.4	17.4	6.5	<0.01
JMG-04	And. <sup>arg.</sup>	27.9	102.5	108.2	463.1	61.8	<0.01	25.4	4.2	<0.01
JMG-05	And. <sup>prop.</sup>	8.1	101	427.6	374.2	286.1	1.5	18.3	5.5	<0.01
JMG-06	And. <sup>prop.</sup>	11.6	101.2	22.9	237.6	929.9	4.2	27.8	14.1	<0.01
JMG-07	And. <sup>arg.</sup>	78.2	101.9	38.2	40.9	61.2	1.1	12.8	4.6	<0.01
JMG-08	And. <sup>prop.</sup>	13	103.8	33.7	31.9	67.4	<0.01	12.9	4.2	<0.01
JMG-09	And. <sup>arg.</sup>	32.7	102	221.5	491.9	82.1	0.4	20.8	4.4	<0.01
JMG-10	And. <sup>si.</sup>	54.3	101.4	1827.1	155.5	449.6	2.3	11	4.4	2.4
JMG-11	And. <sup>arg.</sup>	35.5	102.2	354.1	27.7	151.9	2.3	14.5	7.9	<0.01
JMG-12	Volc. Breccia	129.2	101.4	42.1	535.3	541.2	4.1	16.8	16.9	0.8
JMG-13	And. <sup>prop.</sup>	9	101.5	449.5	447.4	266.7	1.6	15.8	5.6	<0.01
JMG-14	And. <sup>arg., sulph.</sup>	15.8	101.1	21.2	117.7	233.6	0.8	11.3	4.8	<0.01
JMG-15	And. <sup>arg., sulph.</sup>	13.2	101.3	9.1	19.6	65.1	<0.01	12	4.5	<0.01
JMG-16	And. <sup>arg., sulph.</sup>	11.8	101.2	13	12.2	73.9	<0.01	12.4	5	<0.01
JMG-17	And. <sup>arg., sulph.</sup>	14	101.4	15.4	27.6	130.3	0.4	19.7	13.9	<0.01
<b>Minimum</b>		8.1	101	9.1	12.2	61.2	<0.01	11	4.2	<0.01
<b>Maximum</b>		129.2	103.8	1827.1	535.3	929.9	4.2	27.8	16.9	2.6
<b>Average*, <math>\bar{x}</math></b>		30.6	101.7	254.0	236.9	232.9	1.4	16.2	6.3	2.5

Remarks: Alt = alteration, And = andesite, arg. = argilised, prop. = propylitised, si. = silicified, sulph. = sulphidised, bdl = below detection limit, \* = average exclude of volcanic breccia.



Cu, Pb and Zn have no variation with andesite alteration profiles, but As does, as it is relatively higher in argillised and silicified andesite and volcanic breccia than in propylitised andesite. Also, Zn appears to be sorbed onto secondary minerals ( $r=0.98, 0.86, \text{ and } 0.88$ , with respect to  $\text{SiO}_2$ ,  $\text{Al}_2\text{O}_3$  and  $\text{Fe}_2\text{O}_3^T$ ) (Table 5) than other trace elements, indicating its high susceptibility to sorption by secondary minerals. Ba, Cd, Cr, Ni and Ag made up the relatively less significant, and their concentrations are  $101.0\mu\text{g/g} - 103.8\mu\text{g/g}$ , below the detection limit to  $4.2\mu\text{g/g}$ ,  $11.0\mu\text{g/g}$  to  $27.8\mu\text{g/g}$ ,  $4.2 \mu\text{g/g}$  to  $16.9\mu\text{g/g}$ , and below the detection limit to  $2.6\mu\text{g/g}$ , respectively. These suggest their concentration in parent rocks is lower and could have a minimum impact.

**Table 5. The coefficient of correlations,  $r$  between  $\text{SiO}_2$ ,  $\text{Fe}_2\text{O}_3^T$ ,  $\text{Al}_2\text{O}_3$  with trace elements in weathered andesite.**

Item	As	Ba	Cu	Pb	Zn	Cd	Cr	Ni
$\text{SiO}_2$	0.43	0.04	-0.35	-0.44	-0.98	-0.03	0.22	-0.58
$\text{Al}_2\text{O}_3$	-0.16	-0.27	0.31	0.32	0.86	0.13	-0.47	0.38
$\text{Fe}_2\text{O}_3^T$	-0.47	0.28	0.03	0.52	0.88	-0.35	0.12	0.40

Remarks: calculated for samples JMG-01, JMG-04, JMG-07, JMG-08, JMG-11 and JMG-13, where secondary minerals appeared in XRD spectrograms.

## CONCLUSION

Hydrothermal activities appear to influence the geochemical composition of parent rocks and the distribution and abundance of various minerals, such as pyrite and silicate minerals. Upon weathering, they both generate and consume acid. The significant concentration of sulphides, particularly associated with the widespread occurrence of pyrite, indicates a greater potential for acidity generation and, consequently, the release of numerous constituents, especially Cu, Pb, Zn and As, which have a substantially high concentration in the host rocks.

## ACKNOWLEDGEMENT

I am thankful for the assistance provided by Mr Shamsul Arif Haruna, Mr Sze To Han Suon, Mr Edwin James and the rest of the technical team from Southsea Gold Sdn. Bhd. during the fieldwork. Special thanks are also extended to Mr Edwin James for his geologic field interpretation and optical micrographs of hydrothermally altered andesite thin sections specimens. Also, much appreciation is given to Dr Rashita binti Abd Rashid, Ms Norin Safrina binti Mustaffa Kamal, and Mr Sharizan bin Hashim on XRD and XRF analyses conducted at the Mineral Research Centre and Geochemical Laboratory Services of the Department of Mineral and Geoscience Malaysia.

## REFERENCES

- Clark, C. M., & Downs, R. T. (2004). Using the American Mineralogist Crystal Structure Database in the Classroom. *Journal of Geoscience Education*, 52(1), 76–80.  
<https://doi.org/10.5408/1089-9995-52.1.76>

- Downs, R. T., & Hall-Wallace, M. (2003). Using the American Mineralogist Crystal Structure Database. *American Mineralogist*, 88, 247–250. <https://doi.org/10.5408/1089-9995-52.1.76>
- Haruna, S. A. (2016). *Geology and Mineral Exploration in the Bukit Mantri Gold Prospect, Wullersdorf Area, Tawau District*.
- Mackenzie, W. S., Adams, A. E., & Brodie, K. H. (2017). Rocks and Minerals in Thin Section. In *Rocks and Minerals in Thin Section* (2nd Editio). CRC Press. <https://doi.org/10.1201/9781315116365>
- Musta, B., Soehady, H. F. W., & Tahir, S. (2008). Geochemical characterization of volcanic soils from Tawau, Sabah. *Bulletin of the Geological Society of Malaysia*, 54, 33–36. <https://doi.org/10.7186/bgsm2008006>
- Nordstrom, D. K. (2011). Hydrogeochemical processes governing the origin, transport and fate of major and trace elements from mine wastes and mineralized rock to surface waters. *Applied Geochemistry*, 26(11), 1777–1791. <https://doi.org/10.1016/j.apgeochem.2011.06.002>
- Nordstrom, D. K., & Alpers, C. N. (1999). Geochemistry of acid mine waters. In G. S. Plumlee & M. J. Logsdon (Eds.), *The Environmental Geochemistry of Mineral Deposits, Part A. Processes, Techniques, and Health Issues: Society of Economic Geologist, Reviews in Economic Geology* (Vol. 6).
- Plumlee, G. S. (1999). The Environmental Geology of Mineral Deposits. In G. S. Plumlee & M. J. Logsdon (Eds.), *The Environmental Geochemistry of Mineral Deposits, Part A. Processes, Techniques, and Health Issues: Society of Economic Geologist, Reviews in Economic Geology* (pp. 71–116).
- Smith, K. S. (1999). Metal Sorption on Mineral Surfaces: An Overview with Examples Relating to Mineral Deposits. *Review in Economic Geology*, 6A-6B, 161–182. <https://doi.org/10.1.1.371.7008>
- Tahir, S., Musta, B., & Rahim, I. A. (2010). Geological heritage features of Tawau volcanic sequence, Sabah. *Bulletin of the Geological Society of Malaysia*, 56(56), 79–85. <https://doi.org/10.7186/bgsm2010012>
- Winter, J. D. (2014). *Principles of Igneous and Metamorphic Petrology* (Pearson Ne). Pearson Education Limited.
- Yan, A. S. W. (1991). *Features of volcanic-hosted epithermal gold mineralization in the Nagos and Mantri areas, Sabah. Report No. SB 91/1*.